Thermal and spectral impact of building integrated Mirrored Light Pipe to human circadian rhythms and thermal environment

Bruno Malet-Damour, Ali Hamada Fakra

Submission of a manuscript to International Journal of Sustainable Energy

---

Thermal and spectral impact of building integrated Mirrored Light Pipe to human circadian rhythms and thermal environment

---

Bruno MALET-DAMOUR and Damien Ali Hamada FAKRA

Contents:

Corresponding author:
Bruno MALET-DAMOUR
Physics and Mathematical Engineering Laboratory for Energy, Environment, and Building (PIMENT)
University of La Reunion,
117, rue du Général Ailleret
97430 Le Tampon (France)
tél: 06 92 403 906
email: bruno.malet-damour@univ-reunion.fr

Thermal and spectral impact of building integrated Mirrored Light Pipe to human circadian rhythms and thermal environment

Bruno MALET-DAMOUR[1]* and Damien Ali Hamada FAKRA[2]

University of La Reunion, Physics and Mathematical Engineering Laboratory for Energy, Environment and Building (PIMENT)

120, rue du Raymond BARRE 97430 Le Tampon, France.

1 : bruno.malet-damour@univ-reunion.fr / ORCID : 0000-0001-8216-265X

2 : fakra@univ-reunion.fr / ORCID : 0000-0002-6069-9015

Highlights

- A short review on experimental and numerical thermal results on Mirrored Light Pipe (MLP)
- New experimental observations for the thermal aspect of MLP in high solar potential climate
- Evaluation of the MLP efficiency on human circadian rhythms

Abstract

Light holds an important place in the way of life of humans. The first type of lighting which could be exploited was daylight. Tubular Daylight Guidance Systems (TDGS) transport and distribute this daylight inside a building. This article focuses on one of the best known: the Mirrored Light Pipe. MLPs are multiple specular reflectance transporters.

This paper presents (i) state of the art on thermal and spectral studies on light pipes from 1998 to 2021 and (ii) proposes an experimental analysis on MLP in the climatic environment with a high solar resource for different spectral bands of the daylight spectrum. The results show that the thermal impact of the light pipe is limited. Moreover, it is demonstrated that this device promotes natural circadian rhythms. A comparison with artificial lighting highlights this device as an ideal solution for bioclimatic building design.

Keywords: Building applications ; building design ; daylight performance ; daylight ; circadian rhythm ; thermal conditions ; spectral characterization

Nomenclature

τ_{TDGS}	*Transmission coefficient of the light pipe*	*[-]*
ρ_{LP}	*Internal reflectivity coefficient*	*[-]*
Ap	*Aspect ratio* $Ap = {Length_{LP}}/{Diameter_{LP}}$	*[-]*
$I_{G,out,h}$	*Outdoor global irradiance*	*[W/m²]*
$I_{d,out,h}$	*Outdoor diffuse irradiance*	*[W/m²]*
$I_{G,in,h}$	*Indoor diffuse irradiance*	*[W/m²]*
$L_{D,out}$	*Outdoor downward longwave radiation*	*[W/m²]*
$L_{D,in}$	*Indoor downward longwave radiation*	*[W/m²]*
$L_{net,out}$	*Outdoor net radiation*	*[W/m²]*
$L_{net,in}$	*Indoor net radiation*	*[W/m²]*
SR	*Sky Ratio*	*[-]*
λ	*Wavelength*	*[nm]*
ϕ_v	*Luminous flux*	*[lm]*
ϕ_e	*Radiant flux*	*[W]*
η	*Luminous efficacy*	*[lm.W⁻¹]*
LP	*Light pipe*	*[-]*
LW	*Long-wavelength*	*[-]*

Introduction

Today, humans spend nearly 90% of their time in indoor environments [1]. This environment, particularly in the thermal and luminous domains, is far from how the human species developed and set up its mechanisms of adaptation and physiological regulation. To create interior spaces adapted to human health, daylighting technologies must be exemplary: limited heat input and conservation of the properties of transmitted light. Although less and less energy-consuming, artificial lighting is often at the origin of chronobiological regulations modulated by a hormone: melatonin. The color temperature of light sources, whether natural or artificial, affects user performance. The higher the color temperature (towards white), the higher the performance [2]. This is related to the increase in vigilance caused by the inhibition of the nocturnal secretion of melatonin. Recent studies show that they are linked to the direct activation of brain structures involved in cognition, wakefulness and sleep regulation, and circadian rhythms [3]. Concretely, insufficient or inappropriate exposure to light can disrupt traditional human rhythms, with adverse consequences on cognitive performance, comfort, and health [4–6].

The many existing international Tubular Daylight Guidance Systems [7] are among those devices that meet both energy and health criteria. They allow the transport and distribution of daylight into dark rooms, away from traditional openings. Previous work [8,9] has shown the photometric performance of the light pipe

in extreme sunlight situations (maximum global illuminance of about 200 Klux). Moreover, they seem to offer the advantage of minimizing light loss and heat gain while guaranteeing that the light retains all its health-related properties. However, although mirrored light pipe seems to transmit less solar infrared (heat) than visible light, few experimental studies have confirmed this.

This paper presents observations from experiments conducted over 2018-2019 on Mirrored Light-Pipe (MLP) in Reunion Island, France. The climate in which the investigation was undertaken is presented with a focus on solar irradiance. In 2021, this study is the only one to analyze the thermal impact of this type of device in a tropical climate with extreme sunlight conditions. The experimental results, differentiated by the sky typology, allow to qualitatively analyze the impact of the light pipe on (i) the infrared transmission, (ii) the energy flux effectively transmitted, and (iii) measure the profile of the electromagnetic spectrum at the device exit. This last study allowed (i) to evaluate the shape of the solar spectrum and its impact on human perception and (ii) to compare the wavelength of the light pipe to that of the main artificial lighting.

1. A short review on thermal and spectral light pipe investigations

1.1. Light spectrum transmitted by the light pipe

The luminous intensity of a source and the color of the transmitted light has an important impact on the perception of ambiance. It is generally assumed that spectral variations generated by reflective light pipes do not affect the color of the transmitted daylight. In 2014, Nilsson et al. [10] confirmed this assumption. To do so, they use a numerical approach and spectrophotometric measurements (controlled environment) to qualify the illuminances (direct/diffuse) entering inside the pipe, neglecting the presence of the collection and diffusion device. The MLP appears to have achromatic properties. The author also states that the spectroscopic behavior may depend on the aspect ratio of the light pipe. It is also noted that the angle of incidence of the incoming beam affects the spectral transmittance of the tube. Low angles of incidence (less than 50°) allow rays of length between 400 and 800 nm (visible) to penetrate. The angles of incidence up to 50 ° extend the spectrum of rays: from 400 to 1000 nm (visible + near IR).

In 2000, Shao and Riffat conducted an experimental study in England (real environment, northern hemisphere, max illumination: 20 Klux) on a system combining light pipe and passive thermal ventilation [11]. Part of their study showed that this system transmitted (slightly) less IR than visible light. Under cloudy skies, IR radiation is about three times less and more uniform than under clear skies.

In 2003, Callow [12] studied mirrored light pipes and another type of light pipe (light rods) for two different real-world climatic environments: England (temperate oceanic climate, max illuminance: 80 Klux) and Singapore (equatorial climate, max illuminance: 120 Klux). He showed that the light rods (based on fiber optics) could provide more significant amounts of light without compromising the thermal performance of the building. The transmission properties of the PMMA material that constitutes the light rods (but also the collector of the MLP) favor the transmission of visible and near-infrared wavelengths but effectively limit the mid-infrared and beyond, which was confirmed by the study of Nilson [10].

In 2019, Omishore [13] experimented with a light pipe prototype associated with an active collection device (parabolic collector with concentrating mirror). The device is subjected to an artificial IR light source (controlled environment). The author then records the temperature profiles and takes thermographic pictures. The temperature measurement data show a significant increase in the temperature at the surface of the light pipe in response to the IR radiation. The author indicates that the light pipe could be supplemented with an additional vented pipe to prevent any overheating problems, which has been confirmed by other authors [14–18].

1.2. Impact on indoor thermal conditions and study of solar heat gain

The thermal behavior of a light pipe in a real-world environment has been little studied, and even less in tropical climatic conditions. The literature referenced only one author, Williams [19] in 2014. Through an experimental study in a real environment, the author investigated the photometric and thermal behaviors of the device for two types of the day (clear and overcast) for a seminar room located in Kingston, Jamaica (northern hemisphere). The results show a significant temperature gradient during the day, increasing the energy consumption of an active cooling system to maintain a comfortable temperature of 25°C. Indeed, on a clear day, the diffuser was 6.68°C warmer than the ambient temperature, and the collector was nearly 4.45°C warmer than the diffuser. At night, the author shows that the light pipe behaves as a thermal bridge because the temperature of the dome is always lower than the temperature of the diffuser and the room.

In another climatic context (measurement in a real Canadian environment), Harrison [20], in 1998, conducted a thermal study of a commercial light pipe measuring 0.33 m in diameter by 1.83 m in length. A winter period was chosen. His experiment reported an average effective thermal resistance of 0.279 $m^2.K.W^{-1}$. However, this value reflects a measurement of the outside air temperature to the inside air temperature.

Other authors [12,21–27] have also attempted to understand the thermal impact of the type of light pipe and its geometric characteristics, the modes of heat transfer, and the influence of climate. Overall, although the device has a limited impact on thermal conditions, the ratio of light input to heat input is still attractive. The heat input generated by the light pipes has a lower impact than the artificial lighting.

1.3. Stack ventilation with light pipe and CFD Study

Several authors have been interested in studying the light pipe associated with a thermal draft [14–18]. In single or double tubes, the light pipe is tested to quantify the impact it could have on natural ventilation. In double tubes, the temperature rise of the inner tube walls is limited by the convective phenomena occurring in the outer tube. The authors have demonstrated a definite potential to couple these two phenomena through numerical simulations in fluid dynamics or experimental measurements (temperature profiles).

1.4. The originality of the paper

The studies reviewed in the literature from 1998 to 2021 report thermal and spectrometric findings summarized and classified by theme in Table 1. These different observations were conducted in a real environment (temperate, equatorial, or tropical climates) or controlled (laboratory measurements) and exclusively in the northern hemisphere. For tropical countries, the use of daylighting technologies is a significant concern because of the heat associated with sunlight, which can increase the cost of cooling, thus reducing the energy savings resulting from the reduction of the lighting load. This paper presents the only experimental data in the southern hemisphere (different solar path) and for extreme sunlight conditions. Under these climatic conditions, we come to refute, confirm or bring a new perspective on the impact of the Mirrored Light Pipe on thermal and spectral conditions, its impact on natural human biological rhythms.

After an annual analysis of the solar irradiation of the study site (St-Pierre, LA REUNION, southern hemisphere) to identify the extreme climatic conditions, we oriented our approach by proposing measurements on several spectral bands of daylight (see Figure 1). We sought to confirm that, despite the intense solar radiation, the light pipe brings little IR GLO (pyrgeometer measurements), that the thermal effect of the transmitted energy remains low compared to the visible part (pyranometer measurements), and that the wavelength spectrum of the penetrating radiation (i) is close to the spectrum of the sunlight, to the benefit of the suppression of UV (responsible for the aging of the materials) (ii) and of better quality than any artificial lighting. We associate our spectroscopic analysis to the quality of the transmitted light about its adequacy with the natural biological (circadian) human rhythms.

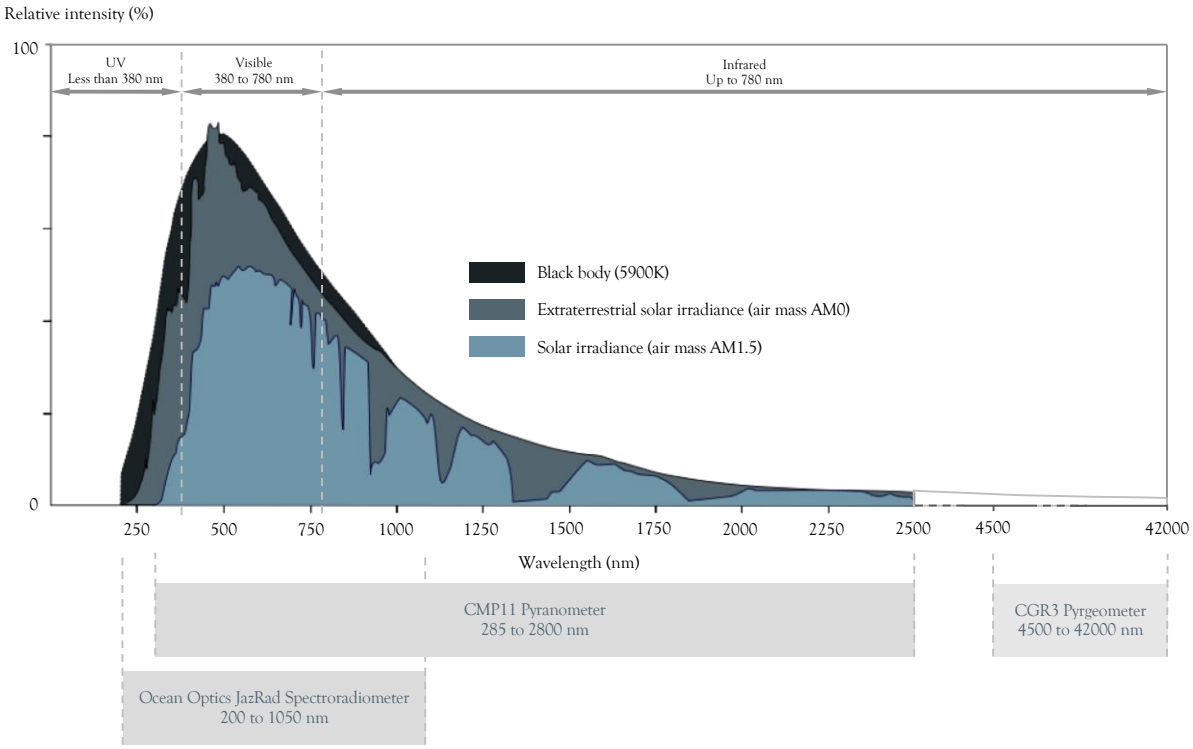

Figure 1: Measurements made in the course of this work

All these results represent a further advance in understanding the behavior of tubular mirrored daylight guidance systems and contribute to the continuous improvement of this technology.

Table 1: synthesis of numerical and experimental studies from 1998 to 2020

Reference	Findings
Light spectrum transmitted by the light pipe MLP	
Nilsson et al. [10]	Achromatic properties
	Spectroscopic behavior depends on the aspect ratio
	The angle of incidence affects the spectral transmittance: (i) less than 50°: wavelengths between 400 and 800 nm (visible); more significant than 50°: from 400 to 1000 nm (visible + near IR)
Shao and Riffat [11]	Under cloudy skies, the number of IR rays is about three times lower and more uniform than under clear skies
Callow [12] Nilson et al. [10]	PMMA (collector material) favors the transmission of visible and near IR wavelengths while effectively limiting the medium and far IR
Omishore [13]	Significant increase in the surface temperature of the light pipe in response to IR radiation
Impact on indoor thermal conditions and study of solar heat gain	
Williams [19]	An only experimental study in tropical climatic conditions (northern hemisphere)
	Large temperature gradient during the day
	Thermal bridge at night
Harrison [20]	The average effective thermal resistance of 0.279 $m^2.K.W^{-1}$ for a light pipe with Ap = 5.55
Callow [12], Callow [21], Laouadi [22], McCluney [23], Bencs [24], Perčić [25], Hien [26], Wu [27]	The heat contribution of a light pipe is lower than artificial lighting
Stack ventilation with light pipe and CFD study	
Varga [14], Oakley [15], Šikula [16], Šikula [17], Ait-taleb [18]	Interesting coupling of thermal draft + light contribution
	Double ducting limits the temperature rise of the reflective surface

2. Materials and methods

Reunion Island is very particular because of its high solar irradiation. As we have seen in a previous study [8] and confirmed by the literature, it is necessary to study the environment of the light pipes to understand their behavior. For this reason, we have chosen to set up an experiment to verify and validate the literature observations. Three experimental objectives have been identified:

- Objective 1: Analyze the annual solar irradiation profile of the experimental site to understand the profile of the available solar resource,
- Objective 2: Measure the profile of the wavelength of the light effectively transmitted by the light pipe by highlighting the filtering effect of the device for two types of day,
- Objective 3: Evaluate the device's potential for the human circadian cycle compared to traditional artificial lighting sources.

Thanks to the results of the experiments set up, we will understand the impact of the light pipe on the interior ambient conditions and the comfort of the individual.

2.1. Experiment set-up

The study support is an experimental cell of 9m^2 located in Saint-Pierre (Reunion Island). This cell is oriented North/North-West (9° N) and positioned on a platform without any distant mask impacting the cell. The dimensions of the test cell are described in Figure 2. The vertical walls are made of composite panels (fibrocement/polyurethane/ fibrocement), and the horizontal ceiling is made of wood. Each interior face is covered with 5 cm of white polystyrene to reduce the radiative effect. The sloping roof (20°) is made of midnight blue corrugated sheet metal. A mirrored light pipe (ρ_{LP} = 99.7%; Ap = 4.6) of the brand SOLATUBE® was installed in the roof plane. It is curved to ensure the horizontal of the diffuser.

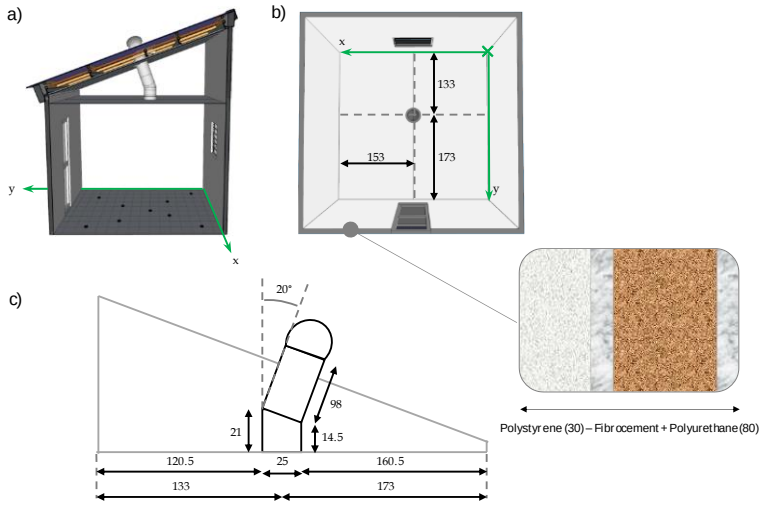

Figure 2: a) Cross-section view of the LGI cell b) Bottom view of the LGI c) Dimensions of the light pipe

2.2. Measurement & data acquisition

To meet each of the established objectives, we wished to set up different studies.

2.2.1. Measurements of short wavelength from pyranometer sensor

Two CMP11 pyranometers are used to measure most solar radiation (285 to 2800 nm) and mainly short wavelengths. These measurements offer elements of response to objectives 1 and 2. To answer the objective N°1, it was necessary to obtain a complete year of measurement to put forward the seasonal profile of the place of study by using two pyranometers (global and diffuse radiation). Then, to answer partly to the objective N°2, wishing to identify the filtering effect of the light pipe, we used two pyranometers. One is placed directly under the diffuser with a black plastic cap, and the other is placed outside in the plane of the sensor (Figure 3). Since this instrument is intended for outdoor measurements, its sensitivity is relatively high for indoor measurements (7 W/m2). However, we wish to use the same instruments to have the same sensitivity wavelengths (285 to 2800 nm). In this case, failing to quantify rigorously, we adopt a qualitative approach "binary." If the transmitted energy is close to the sensitivity, the measurement will show that the light pipe transmits (1) or does not transmit (0) energy. If the measured data are low (close to the sensitivity), the experiment will demonstrate that the device transmits little energy in the spectral range of the pyranometer.

Figure 3: Outdoor pyranometer CMP11 for global irradiance in the plan of the light pipe

The devices are connected to a CAMPBELL SCIE® brand data acquisition system and are synchronized with each other. They record in one-minute time steps, like the scanning.

The pyranometer specifications are given respectively in Table 2.

Table 2: Pyranometer specifications

		Accuracy
Spectral range λ	*285 to 2800 nm*	
Non-linearity	*100 to 1000 W/m²*	*<0.2%*
Temperature dependence	*-40 °C to +40 °C* *+40 °C to +80 °C*	*< 5 %* *< 10 %*
Zero offset	*< 7 W/m²*	
Non-stability (change/year)		*< 0.5 %*
Sensitivity	*7 to 14 µV/W/m²*	
Operating temperature	*-40°C to 80°C*	
Maximum irradiance	*4000 W/m²*	

2.2.2. Measurements of long-wavelength from pyrgeometer sensor

To pursue objective N°2, two CGR3 pyranometers (Campbell Scientific®) were used to evaluate the global irradiation for the spectral band 4500 nm – 42000 nm (thermal effect). The installation methodology is the same as with the pyranometers. The first is placed under the diffuser with a black plastic cap and polystyrene insulation to reduce the radiative effect of the cell walls, which are themselves insulated (Figure 4.a). The second is placed on the roof in the plane of the device collector (Figure 4.b).

As with the pyranometers, the pyrgeometers are devices for measuring in an outdoor environment, with a sensitivity of about 5 W/m^2. To perform the most rigorous study possible on the effect of the light pipe, the outdoor and indoor sensors must have the same spectral bands (4500 nm - 42000 nm). The sensitivity of this sensor may be close to the values recorded indoors; the measurement must be qualitative, like the study with pyranometers. In this case, failing to quantify rigorously, the qualitative binarized approach will show that the light pipe transmits (1) or does not transmit (0) energy on the spectral interval 4500 nm - 42000 nm. If the measured indoor data are low, the study will show that the light pipe transmits little long wavelengths.

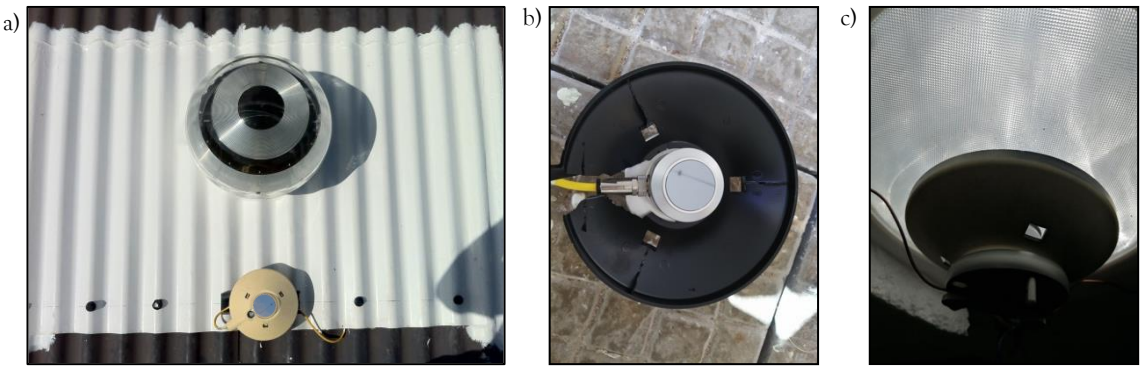

Figure 4: a) outdoor pyrgeometer CGR3 for global irradiance in the plan of the light pipe b) indoor pyrgeometer CGR3 with black protection and insulation provided by polystyrene c) sensor positioned on the light pipe diffuser

As for the pyranometers, the pyrgeometers are connected to a CAMPBELL SCIE® data acquisition system and synchronized. The time step and the scanning are also of the order of one minute.

The pyrgeometer specifications are given respectively in Table 3.

Table 3: Pyrgeometer specifications

		Accuracy
Spectral range λ	*4500 to 42000 nm*	
Non-linearity	*-250 to 250 W/m²*	*<1%*
Temperature dependence	*-40 °C to +40 °C* *+40 °C to +80 °C*	*< 5 %* *< 10 %*
Zero offset	*dT = 5 K/h*	*< 5 W/m²*
Non-stability (change/year)		*< 1 %*

2.2.3. Spectrophotometer utility in the experiment

This study aims to bring elements of the answer to the objective N°3, seeking to establish the electromagnetic spectrum profile transmitted by the light pipe. In addition, it is a question of understanding the role that the light pipe can play on the visual comfort of the occupant and its circadian efficiency. A spectrophotometer was used to measure the electromagnetic spectrum profile at the entrance and exit of the light pipe. The spectrometric measurements are performed by an Ocean Optics® spectrophotometer, model JAZ (Figure 5).

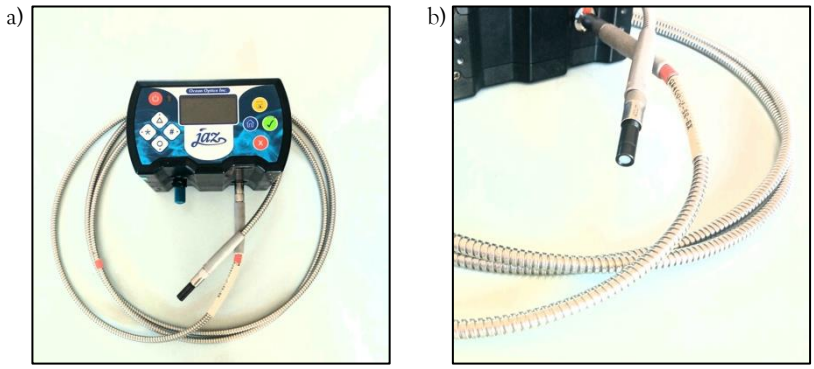

Figure 5: a) Ocean Optics® spectrophotometer, model JAZ for spectrometric measurements in the plan of the light pipe b) Photosensor cell of the spectrophotometer

This apparatus allows measuring the UV/Visible part of an electromagnetic source. The measurement was performed in 2 quasi-synchronous phases: first, the spectrophotometer cell was placed orthogonally under the diffuser. The cell device was placed outside in the plane of the collector. The recording was instantaneous. The specifications of the spectrophotometer are given in Table 4.

Table 4: Spectrophotometer specifications

Description	*Jaz UV/Visible Spectrophotometer with Remote Probe*
Grating options	*14 different gratings, UV through short-wave NIR*
Detector	*2048-element linear silicon CCD array; L2 collection lens*
Spectral range λ	*200 to 1100 nm*
Signal-to-noise ratio	*250:1*
Integration time	*870 μS to 65 seconds*

2.2.4. Summary of the experiments conducted

All experimental scenarios were synthesized in Table 5.

Table 5: Experimental scenarios

N°	***Period used***	***Measurement***	***Sensors***	***Objectif***
1	*1 year (2019)*	$I_{G,out,h}$ $I_{d,out,h}$ $I_{G,in,h}$	*3 x CMP11 pyranometers*	*Quantitative approach :* Annually solar resource for brief climate study
	3 days (April 2018)			*Qualitative approach : Evaluate the ability of the light pipe to transmit radiation in the spectral band (285 to 2800 nm) for 3 types of the sky (clear, overcast, and intermediate)*
2	*3 days (June 2019)*	$L_{net,out}$ $L_{net,int}$ $L_{D,out}$ $L_{D,int}$	*2 x CGR3 pyrgeometers*	*Qualitative approach : Evaluate the ability of the light pipe to transmit IR (4500 nm to 42000 nm) for 3 types of the sky (clear, overcast, and intermediate)*
3	*2 days (October 2019)*	*Outdoor and indoor spectral irradiance (W/m²/nm)*	*1 x JazRad spectrophotometer*	*Quantitative approach : Quantified the outdoor light spectrum in the plan of the collector and the indoor light spectrum under the diffuser for two types of the sky (clear and overcast) for the spectral band (200 to 1100 nm)*

3. Results and discussion

3.1. Annually solar resource for brief climate study

We carry out a brief climatic analysis of the environment in which the light pipe is positioned. The objective is to understand the solar potential of the city of Saint-Pierre, Reunion Island (France). We seek to discern the annual evolution of the global outdoor irradiance measured with an external pyranometer (CMP11).

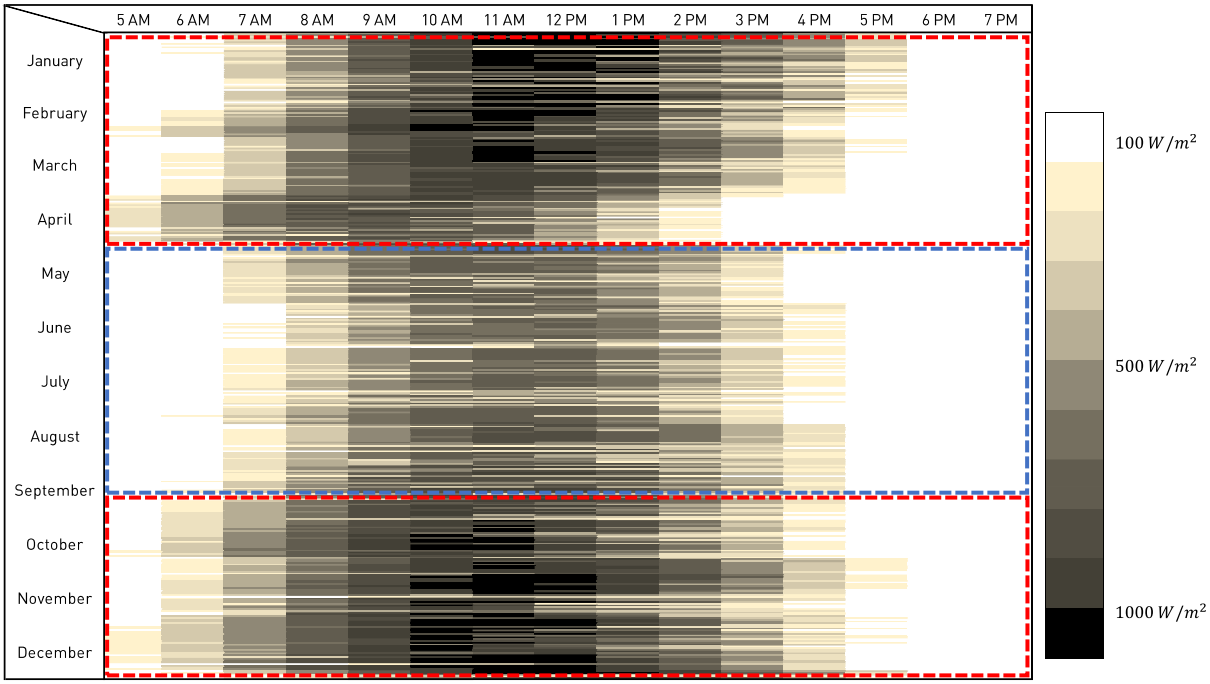

Figure 6: Hourly distribution of $I_{G,out,h}$ for Saint-Pierre (La Reunion, France) during the year 2019

Figure 6 highlights a significant seasonality in global irradiance corresponding substantially to the seasons present in Reunion Island. The southern summer extends from October to April. This is the period when the solar resource is most abundant. The days reach a maximum irradiance frequently between 700 W/m^2 and 900 W/m^2, and, sometimes, up to 1000 W/m^2 (in a clear sky), and the beginning and end of the day close to 200 to 500 W/m^2.

From May to September, the southern winter is the period when the maximum irradiance is around 100 to 800 W/m^2. The days are shorter. Mornings and ends of the days provide less than 200 W/m^2. The trend changes as early as September when the days recover from hours of sunshine.

Indeed, the length of the days also changes according to the season: in the first summer period, the light pipe can benefit from an irradiance of almost 11 hours. In the second period (southern winter), the length of the days is shortened to an average of 9 hours. In the third period (close to the summer solstice), the days are the longest, with more than 12 hours of sunshine.

Seasonality does not seem to be adequately related to the lighting needs. Indeed, a system using daylight within a building will offer significant efficiency from October to April and less for the rest of the year.

3.2. Characterization of day types

Many approaches have been made to characterize the type of sky [28], but few have been made to define typical days. We note in the literature the models of Kittler [29], Perez [30], Perraudeau [31], and a simplified model [32]. The latter is based on the ratio of diffuse to global irradiance. Fakra [33] evaluated the characterization given by these indices over three types of the day (clear, intermediate, and overcast skies). He concludes that the simplified model seems to be more suitable. Apart from sunrise and sunset for each day, the SR index characterizes the day type well overall. We will use this indicator for further experimentation.

The Sky Ratio can be evaluated from the following ratio :

$$SR = \frac{I_{d,\text{out},h}}{I_{G,\text{out},h}} \tag{1}$$

The proposed characteristic values are listed in Table 6.

Table 6: Characteristic values of SR

Type of sky	SR
Clear	$SR \leq 0.3$
Intermediate	$0.3 < SR < 0.8$
Overcast	$SR \geq 0.8$

This characterization will be used to analyze our results according to the different types of days.

3.3. Irradiance through the light pipe (285 to 2800 nm)

The objective of this measurement was to qualitatively assess the magnitude of energy transmitted through the light pipe inside the experimental cell for three typical days (clear, intermediate, and overcast).

Using the SR, we select three typical days: April 3, 6, and 7. The graphs (Figures 7 and 8) that follow are drawn at the 10-minute time step to reduce the impact of climatic contingencies.

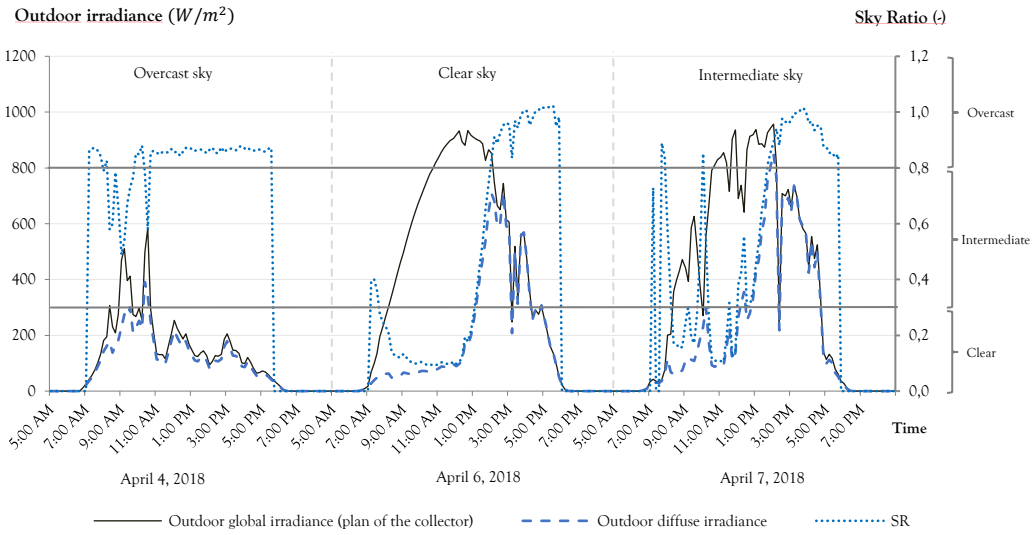

Figure 7: Global ($I_{G,out,h}$) and diffuse ($I_{d,out,h}$) outdoor irradiance for three types of days (4, 6, and 7 April)

April 4 is an overcast day (Figure 7). The global irradiance profile is almost similar to diffuse irradiance, which is typical of a cloudy sky. This classification is confirmed by the SR, which reaches an average value of 0.9. Events appear around 9 AM and 11 AM. They should probably be associated with a partially and momentarily clear sky.

April 6 is considered a clear day, with an average SR of about 0.3. The morning is clear of any clouds (the diffuse irradiance is very low), and scattered cloudy episodes may appear from 3 PM. Like those of April 6, clear sky days are relatively frequent at this time of the year in Reunion Island, where the thermal breeze regime pushes the clouds in the island's heights, which allows clearing the sky for the coastal areas where the tests take place.

April 7 is an intermediate day, confirmed by the average SR reaching 0.4. The global irradiance can reach 900 W/m^2 with drops in irradiation caused by the presence of clouds.

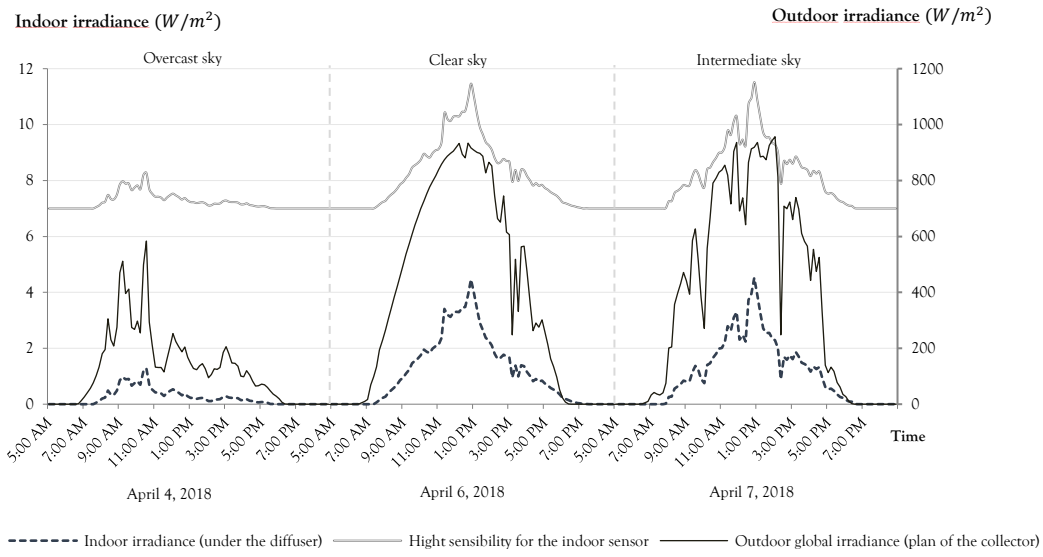

Figure 8: Indoor ($I_{d,in,h}$) and outdoor ($I_{G,out,h}$) irradiance for three types of days (4, 6, and 7 April), and the high sensibility of the indoor sensor

We also plot the indoor and outdoor solar irradiance evolution on the same graph (Figure 8). The indoor irradiance level is low for each day and close to the sensor's sensitivity (±7 W/m^2, for more information about this value, see Table 2). These values do not allow us to give a precise quantity of transmitted irradiance. However, the data collected shows that low intensity is transmitted through the light pipe.

For the overcast day of April 4, the maximum indoor irradiance integrating the sensor's sensitivity is approximately 4.8±7 W/m^2 at 11 AM against 580 W/m^2 outside at the same time or more than 120 times less. For April 6 (clear sky), at 12:50 PM, the nominal global outdoor irradiance is 920 W/m^2 against 7.5±7 W/m^2 indoors, or more than 123 times the transmitted energy. The trend is verified for April 7 (intermediate sky), where the maximum indoor irradiance is close to 8±7 W/m^2 at 12:50 PM against nearly 918 W/m^2 outside. The shape of the interior irradiance curve seems to be different from that of the exterior irradiance. The

specular reflection inside the light pipe must significantly impact the amount of energy transmitted, just as it was noticed for the illuminance in later works [8].

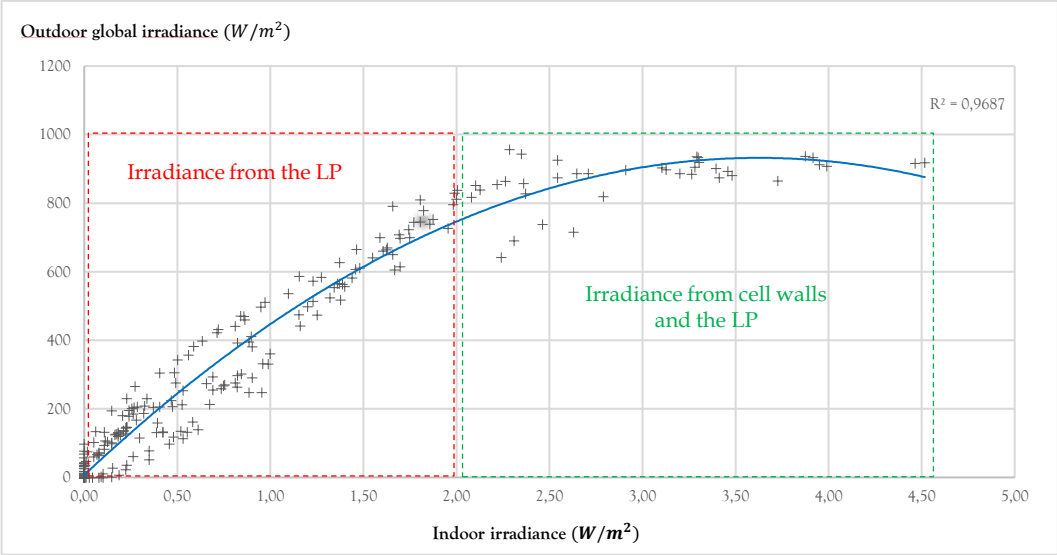

Figure 9: Correlation between outdoor ($I_{G,out,h}$) and indoor ($I_{d,in,h}$) irradiance

When we study the relationship between outdoor and indoor irradiance (Figure 9), we notice a strong positive linear correlation between the two parameters with an R^2 coefficient of 96.9% (see the red frame of Figure 9). The polynomial form of this correlation allows us to understand that the energy contribution by the light pipe is linear up to 780 W/m^2 but grows less quickly beyond. Moreover, the fact that the internal irradiance continues to expand beyond this level indicates the energy transmitted not by the light pipe but most probably by the diffuse thermal interreflection in the inner surface of the cell walls (see the green frame of Figure 9).

These findings allow us to conclude that the energy transmitted by a light pipe in the wavelength range between 285 and 2800 nm is very low, even negligible. This wavelength includes most of the electromagnetic spectrum of light: the visible range and much of the infrared (IR-near). These measurements reveal that the thermal effect, even if it is not finely expressed (related to the sensitivity of sensors), is minimal with the light pipe, compared to a window.

3.4. Estimation of the luminous efficacy of the light pipe

Considering the results obtained in previous work evaluating the nominal luminous fluxes transmitted by the same light pipe for the same climate [9], we can deduce the luminous efficiency of the mirrored light pipe based on the measurements performed in the previous section.

For this, we use the most unfavorable values of the radiant flux (the largest, because of the high sensitivity of the sensor: +7W/m^2), we obtain :

$$\eta_{clear_{min}} = \frac{\phi_v}{\phi_{e_{MAX}}} = \frac{\phi_v}{\phi_{e_{measure,MAX}} + Sensibility_{sensor}} = \frac{6800}{8+7} = \frac{6800}{15} = 453\ lm.W^{-1} \quad (2)$$

$$\eta_{overcast_{min}} = \frac{\phi_v}{\phi_{e_{MAX}}} = \frac{\phi_v}{\phi_{e_{measure,MAX}} + Sensibility_{sensor}} = \frac{710}{4.8+7} = \frac{710}{11{,}8} = 60\ lm.W^{-1} \quad (3)$$

Compared with the types of artificial lighting and their characteristics presented in [9], we obtain Table 7.

Table 7: Comparison of the luminous efficacy of several artificial lighting solutions with those of the light pipe

Light source		*Maximum radiant flux* $\phi_{e_{MAX}}$ *[W]*	*Luminous flux* ϕ_v *[lm]*	*Minimum Luminous efficacy* η_{min} *[lm.W^{-1}]*
Global outdoor irradiance According to [34]				*121.5*
Mirrored Light pipe curved with ρ_{LP} *= 99.7% and Ap =4.6*	*Clear sky*	*15*	*6800*	*453*
	Overcast sky	*11.8*	*710*	*60*
Incandescent bulb		*60*	*710*	*11.8*
Halogen bulb		*70*	*1200*	*17.1*
Compact fluorescent lamp		*23*	*1500*	*65,2*
Traditional fluorescent tube		*56*	*3400*	*60.7*
LED		*3*	*150*	*50*

We note that the luminous efficacy of the light pipe in a clear sky is much better than the other current artificial lighting devices and equivalent to the luminous efficacy of a traditional fluorescent tube in an overcast sky. In the clear sky, despite an estimated radiant flux at the highest (15 W), the light pipe offers a luminous efficiency of about 453 lm.W^{-1}, which is next to 7 times more than the compact fluorescent lamp. Compared with the outdoor luminous efficacy, according to [34], we can see that the low share of thermal energy transmitted in favor of a highly luminous flux allows the light pipe to improve the luminous efficacy of the transmitted daylight.

3.5. Infrared through the light pipe (4500 nm to 42000 nm)

The measurement of this radiation is carried out with a Kipp & Zonen CG4 pyrgeometer sensitive to a spectral range between 4500 nm and 42 000 nm (99% of the energy of the total infrared spectrum).

The pyrgeometer allows measuring the long wavelengths (LW). Its silicon optical window is designed to allow infrared radiation to pass through. An internal thin-film coating prevents short-wave solar radiation from reaching the LW thermopile (cutting off the shortest wavelengths of the solar spectrum). The infrared radiation received at the Earth's surface is emitted by the entire atmospheric column (CO_2, water vapor, clouds, and other particles).

The measurement method is possible (compare outside and inside) because the light pipe has highly reflective walls (ρ_{LP} = 99.7%). Measurement at the diffuser level is thus sustainable because the IR-rays coming from the light pipe will be preponderant compared to the IR-rays coming from the walls of the experimental cell. The latter contribute little to the overall measurement of IR. Indeed, the IR-rays passing through the tube are mainly reflected and therefore reach the sensor cell. In addition, the absorbed and transmitted parts of the radiation are minimized primarily to the thinness of the tube.

L_D is the downward radiation in LW received by the pyrgeometer from the measured object (i.e., in our case, two situations are presented: outdoor, for the sky and, indoor, for the light pipe diffuser). It is the fraction of infrared radiation (infrared irradiance) emitted by the target object. L_{net} (net radiation) represents the radiative exchange between the sensor surface ($\epsilon.\sigma T^4$ with $\epsilon = 1$ if we considered black body case, given by the manufacturer) and the observed object L_D (sky or light pipe).

$$L_{net} = I_{object} - I_{sensor} \tag{4}$$

$$L_{net} = L_D - \sigma.T^4 \tag{5}$$

The sensor interprets L_{net} as the ratio between the voltage delivered by the pyrgeometer and its sensitivity.

L_D being always positive (the flow being always descending), the sign of L_{net} allows giving the direction of the radiative flow, and thus the direction of the exchange. Thus, in theory: when the diffuser is warmer than the collector (scenario of an overcast sky, or a beginning/end of the day), the radiative flux is rising, so the radiation L_{net} is negative (the sensor measuring positive downward). In the clear sky (or at the peak of solar radiation), the diffuser is colder than the collector, the radiative flux is downward, so the radiation L_{net} is positive. In this approach, L_{net} is zero when there is no exchange between the collector and the diffuser.

The curves are presented with a time step of 10mn on 15 hours per day (from 5 AM to 8 PM) for more readability.

a)

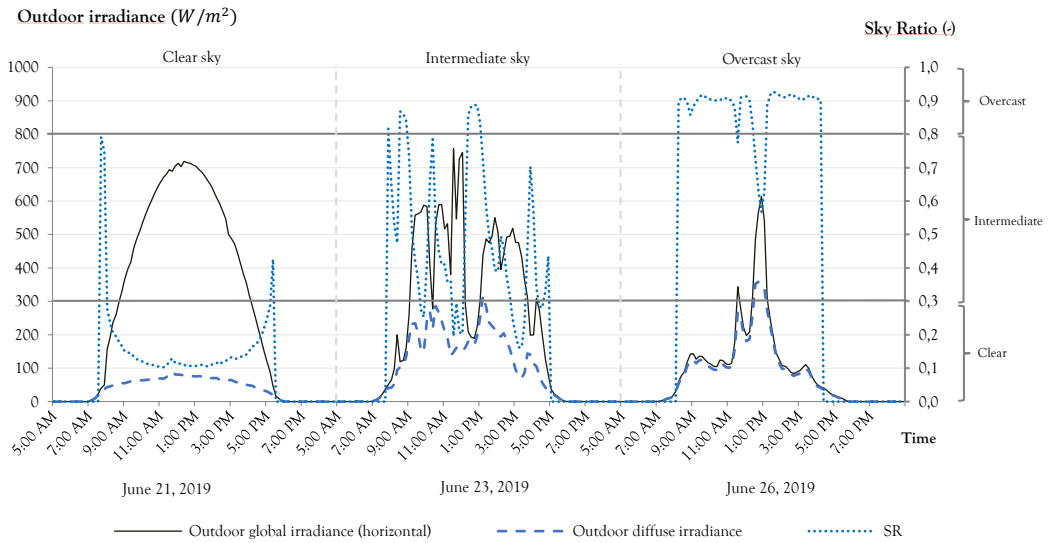

b)

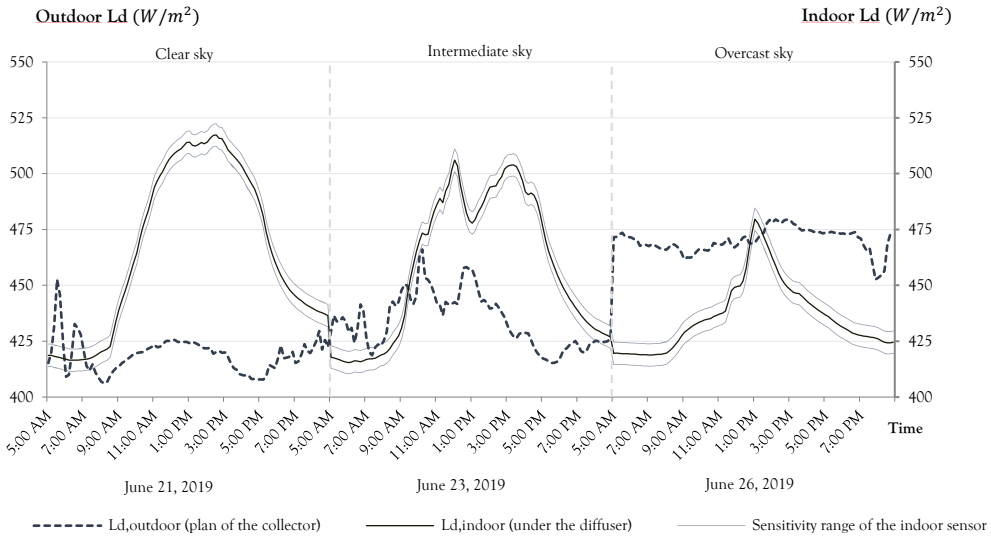

348

c)

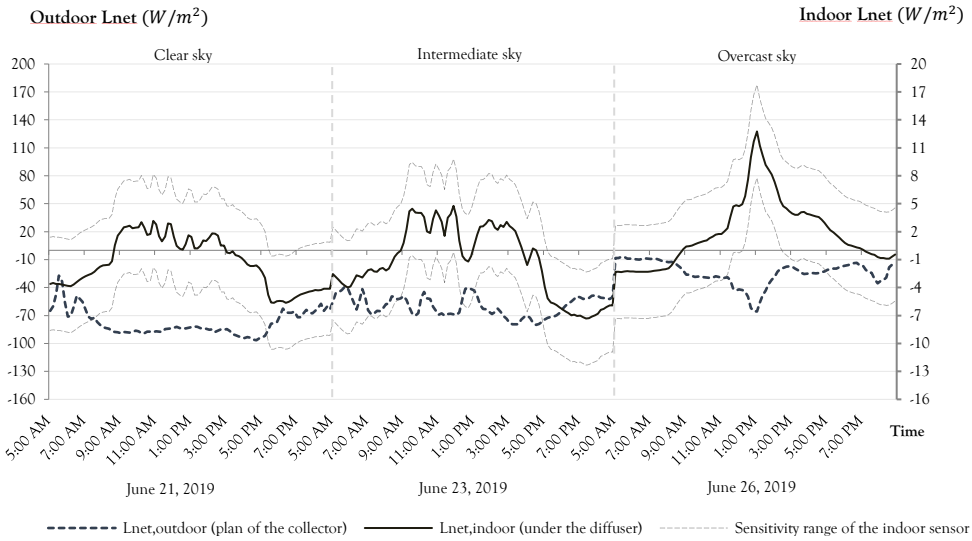

349

350 *Figure 10: a) Global and diffuse outdoor irradiance for three types of days (21, 23, and 26 June) b) Outdoor and indoor*
351 *downward longwave radiation, L_D c) Outdoor and indoor net radiation L_{net}*

352 June 21 (Figure 10.a) is equated with a clear sky day ($SR_{moy} < 0.3$). The high values at the beginning and
353 end of the day are related to this index [33]. The nominal global irradiance measured by an outdoor
354 pyranometer reaches 715 W/m^2 at 12:30 PM. We can see that the downward $L_{D,out}$ radiation at 5:30 AM
355 reaches nearly 450 W/m^2 and then decreases to 407 W/m^2 at 8 AM (Figure 10.b). A parabolic shape is then
356 observed between 8 AM and 5 PM, with a maximum value of 425 W/m^2 reached noon (solar noon, because
357 of the winter solstice in Reunion Island). This observation seems coherent: at the beginning and at the end of
358 the day (when the Sun is not yet visible), there is no radiative exchange between the ground and the sky (i.e.,
359 $L_D = \sigma.T^4$). When the Sun rises and sets, the radiative flux is rising (towards the sky) because the ground
360 temperature increases. The net radiation $L_{net,out}$ is then negative and increases when the ground temperature
361 rises more than that of the sky. Inside the cell and under the light pipe diffuser, the LW $L_{D,in}$ is very high, with
362 a nominal value of more than 520 W/m^2 in the early afternoon (2:30 PM). This can be justified by the fact
363 that the sensor measures radiation from the light pipe elements rather than the sky. As these elements rise in

364 temperature, the infra-reds recorded are those coming from the diffuser and collector. We also note that at the
365 beginning and end of the day, when the diffuser is warmer than the collector, $L_{net,in}$ is negative because the
366 radiative exchange is from the cell to the outside and reverses during the day (Figure 10.c). The values vary
367 between ±3 W/m^2, which is very low, marking the low infrared exchange between the diffuser and the collector.

368 June 23 is an intermediate day (Figure 10.a), confirmed by the SR_{moy} reaching 0.4. The global irradiance
369 can reach 900 W/m^2 with drops in radiation up to 170 W/m^2 at 12:30 PM caused by the presence of clouds.
370 $L_{D,out}$ increases in the presence of cloud masses (Figure 10.b).

371 Finally, on June 26 (Figure 10.a), the profile of the global irradiance is almost similar to that of the
372 diffuse irradiance, which is typical of the evolution of the irradiance during an overcast sky. This classification
373 is confirmed by the $SR_{moy,}$ which reaches an average value of 0.9. $L_{D,out}$ is close to 475 W/m^2, which is consistent
374 with the type of sky. Instead of measuring the radiative exchanges with the sky (colder), the latter measures the
375 radiation of water droplets at air temperature (Figure 10.b). The net radiation $L_{net,out}$ is thus close to zero due
376 to the overcast condition (Figure 10.c). For the net fraction, the difference for long wavelengths is negative and
377 increases during the day. Inside the cell and under the light pipe diffuser, the downward radiation in LW $L_{D,in}$
378 is low, with a nominal value of more than 474 W/m^2 in the early afternoon (1:20 PM). This can be explained
379 by the fact that the angle of incidence is higher. Thus the radiation arrives directly on the sensor, with fewer
380 inter-reflections within the tube. This finding had been noted in the literature for a controlled environment
381 [10].

382 We also note that when the diffuser is warmer than the collector at the beginning and end of the day,
383 L_{net} is negative because the radiative exchange is from the cell to the outside. However, the value reached by
384 L_{net} is wider under cloudy skies than under clear skies, which can be explained by the low-temperature rise of
385 the light pipe components. Moreover, the measured radiation probably corresponds to radiative exchanges
386 with the water droplets trapped in the tube. However, this observation must be modulated because the values
387 reached for $L_{net,out}$ have a reduction factor of nearly ten compared to the outside, with a maximum value of
388 $L_{net,in}$ an overcast sky of about 12 W/m^2, which confirms the weak contribution of IR by the light pipe.

389 Moreover, $L_{D,in}$ presents higher values in the clear sky than in the overcast sky, which translates to an
390 inverse behavior than the one observed in an outdoor environment when the presence of clouds strongly
391 modulates the infrared radiation (emission in the infrared of water drops or ice crystals).

392 **3.6. Spectral irradiance transmitted by a light pipe (200 to 1100 nm)**

393 The objective is to establish the profile of the electromagnetic wave passing through the light pipe for
394 the only two more extreme types of the day (clear sky and overcast sky). With this, we can answer the objective
395 N°2 (to establish the profile of the wavelength transmitted).

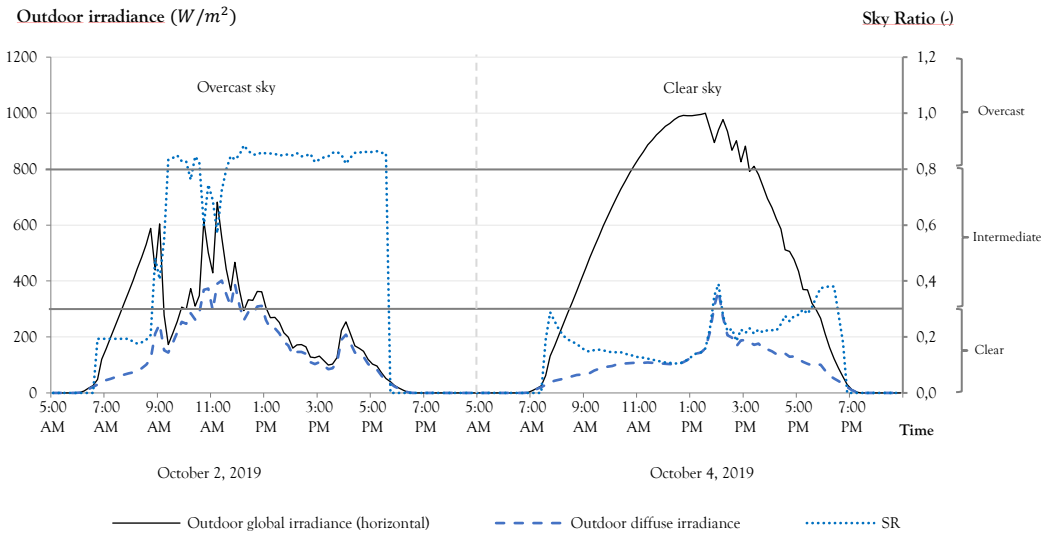

Figure 11: Global and diffuse outdoor irradiance for two types of days (2 and 4 October)

To verify the sky type, we use daily global and diffuse outdoor irradiance (measurements with a CMP11 pyranometer), shown in Figure 11. The first day was October 2, 2019. The sky was overcast (SR > 0.8). At solar noon, irradiance peaked at 300 W/m^2. The second (October 4) was a clear sky with an SR below 0.3. Its irradiance was around 1000 W/m^2.

The measurements with the spectrophotometer were carried out on these two days at solar noon (i) indoors by placing the sensor in the center of the light pipe diffuser and (ii) outdoors, in the plane of the collector, by pointing at the Sun.

The graphs below represent the solar irradiance spectrum at sea level (called AM1.5). We find the atmosphere's absorption bands in the ultraviolet (notably by ozone) and the infrared (notably by water vapor and carbon dioxide).

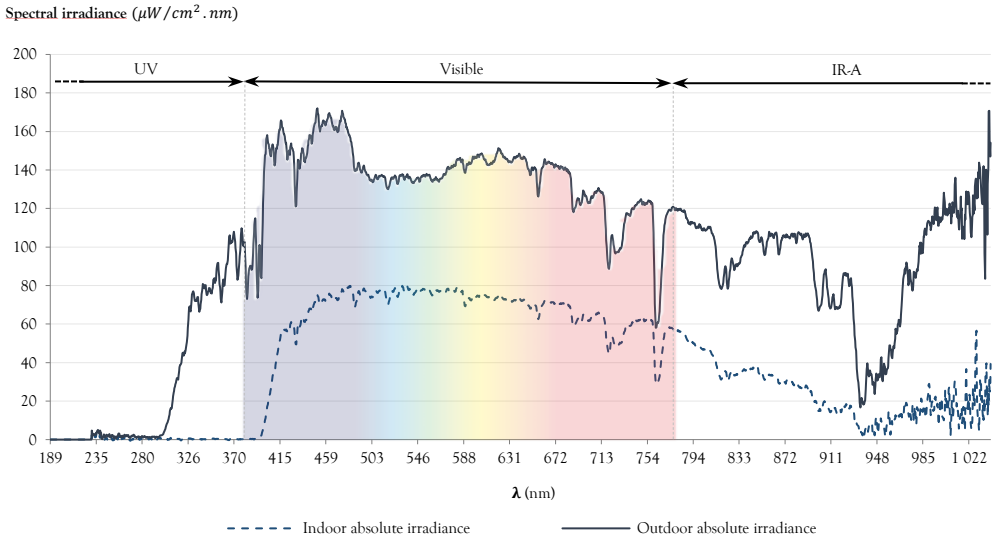

Figure 12: Amount of energy transmitted by wavelength for a day of clear sky (October 4)

In the clear sky (Figure 12) and outside, the profile of the daylight spectrum shows us a relatively continuous spectral irradiance in the visible range. At the exit of the light pipe, no UV is detected. This is probably due to the polymethylmethacrylate (PMMA) properties, which compose the dome of the light pipe collector. This thermoplastic has the advantage of maintaining its transparency, lightness, resistance to UV (responsible for the aging of materials), and corrosion. These properties make it ideal for a collector for a dome subjected to intense mechanical or solar constraints. This same material also seems to act on the near IR, as indicated by Nilson [10] and Callow [12] in their studies.

Regarding the heat input, represented on the graph by the amount of A-IR, we note that the light pipe transmits only a relatively small part of near-infrared (on average, three times less than the external resource) with a substantial decrease beyond 950 nm. This analysis allows us to confirm the results of the literature [11] and the measurements made with the pyrgeometer: the light pipe is only responsible for a small part of the daily heat input. The internal spectral curve also shows that the device smoothes the spectrum of the external electromagnetic wave. The spectral irradiance at the outlet of the device is balanced on each of the visible wavelengths. Our experiment in real weather conditions (i.e., in situ) confirms the results of Nilsson et al. [10] in a controlled environment that the MLP has achromatic properties.

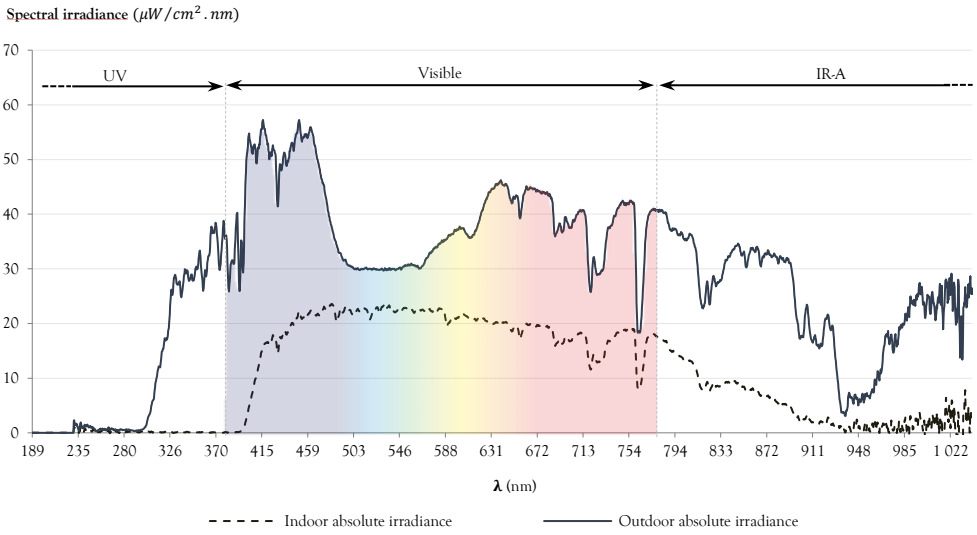

Figure 13: Amount of energy transmitted by wavelength for an overcast day (October 2, 2019)

In overcast conditions (Figure 13), the spectral irradiance values drop by 2 to 4 times compared to the clear sky condition. Outdoors, for UV and IR-A, the electromagnetic waveform remains unchanged. The changes occur mainly for the spectral range 460-630 nm, where the sky absorbs a significant part of the visible spectrum. The profile of the spectrum transmitted by the light pipe remains unchanged compared to the clear sky condition, with a reduction of the amplitude of the spectral irradiance by a factor of 4. This value in a tropical climate is higher but close to the factor of 3 found in temperate climate by Shao and Riffat [11] in their work in a real environment (northern hemisphere, max illumination: 20 Klux).

Based on these findings, it is interesting to compare the spectrum of the electromagnetic wave transmitted by the light pipe with that of artificial lighting devices.

3.7. The efficiency of light pipe on human circadian rhythm compared by artificial lighting

The objective is to compare the spectrum of radiation from the light pipe for two types of the day (clear sky and overcast sky) and from two artificial lighting devices the most used and which we can easily find on the market: LED (T8) and fluorescent lamp (T8). Moreover, this artificial lighting is the most efficient, conforms to Table 7. With this comparative analysis, we can answer objective N°3, namely, to evaluate the concordance of the transmitted light with natural biological rhythms.

Figure 14 is based on the two days explained in the previous section: October 2, 2019 (overcast) and October 4, 2019 (clear). To provide a viable comparison, we normalize the spectral irradiance and smooth the wavelength spectra at scanning of 10 nm.

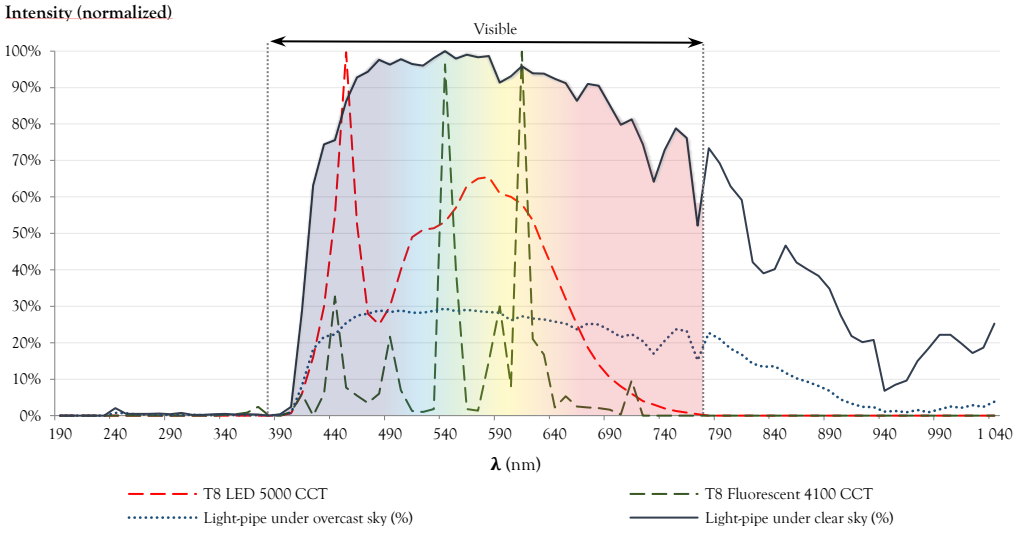

Figure 14: Normalized spectral intensity of the wave: at the exit of the light pipe for two types of the sky; under a LED luminaire (T8 LED 5000 CCT); under a Fluocompact luminaire (T8 Fluorescent 4100 CCT)

The visual system is composed of different biological sensors, photopic (retinal cells: cones and rods), and melanopic (ipRGCs), which ensure, respectively, biological synchronism (chronobiology) and the perception of the environment. The excitation peak of ipRGCs is not the same as that of retinal cells for image formation. It is located between 446 and 480 nm [35] [36] (towards the blue), whereas the nominal efficiency of photopic vision is found at yellow-green wavelengths, close to 555 nm [37]. Thus, the quality of illumination, and more precisely, the wavelength spectrum transmitted, will influence circadian rhythms and cognitive performance. The higher the color temperature (towards white), the higher the performance [2].

Moreover, Cajochen [38] showed that prolonged exposure in the late evening to monochromatic light of 460 nm (blue color) essentially reduced the secretion of melatonin compared to the exact duration of exposure to monochromatic light of 550 nm (green color). The literature [39–45] agrees that circadian rhythms influence cognitive performance: people are more focused and show a progressive improvement during the

biological day, whereas during the biological night, they perform poorly due to temporary attention losses. Therefore, daylight, the most effective stimulus of the master clock, influences the cognitive abilities of human beings.

Our study compares daylight (from the light pipe) and artificial lighting (Figure 14). Whatever the type of sky, the spectrum of the wave coming from the light pipe dominates the blue-green colors while remaining relatively balanced. As we have seen previously, the light from the device is achromatic. The LED has two peaks of intensity: a maximum at 450 nm (blue color) and one at 580 nm (yellow color). This technology has a direct effect on the production of melatonin. Used during the day allows inhibiting the hormone and accentuates vigilance. However, the light issued is monochromatic with bluish dominance, creating discomfort on the color rendering index inside. The spectrum is not complete, so the health benefit is limited. The LED studied should be used in dark spaces, not used at night (scotopic vision). On the other hand, the compact fluorescent lamp emits an irregular and rich spectrum in the green and yellow colors (540 nm and 610 nm), with a value of its spectral intensity low in the blue wavelengths (440 nm). This type of lighting is thus to be proscribed for photopic lighting (daily).

Overall, the experimental results show that the light pipe emits a full spectrum of light in clear and overcast skies. This light favors chronobiological balance and promotes cognitive performance. The intermittence of its luminous flux also allows the occupant to be connected to the climatic variation outside, an important point in the study of visual comfort in the building.

4. Conclusion and perspective

A literature review allowed us to understand that the mirrored light pipe allowed the transmission of achromatic light. Some works have also noted that the transmitted wavelength depended on the angle of incidence of the rays and the aspect ratio. Another finding is that the proportion of IR radiation transmitted is influenced by the type of sky and the kind of material used for the collector. Other studies have revealed that the light pipe, during the night, could work on the thermal environment conditions by acting as a thermal bridge. During the day, the literature notes that this device has only a small heat input, lower than artificial lighting. All the studies reviewed were conducted in temperate, continental climatic conditions and only one in tropical conditions. They are all located in the northern hemisphere.

This paper presents the only experimental data in the southern hemisphere (different solar trajectories) and extreme sunlight conditions. We have aimed to address three distinct objectives: (1) to analyze the annual solar irradiation profile of the experimental location, (2) to measure the spectral profile of the light wavelength effectively transmitted by the light pipe for different spectral bands, and (3) to evaluate the potential of the device on the respect of the human circadian cycle compared to conventional artificial lighting sources.

Several measurements were conducted on different spectral bands to meet these initial objectives, with quantitative and qualitative approaches. The studies are called "qualitative" because of the low values measured indoors, very close to the sensitivity of the sensors. The instruments are thus used to detect flux without

targeting the exact value of the transmitted flux. This approach was applied to measurements in the spectral bands 285 to 2800 nm and 4500 nm to 42000 nm. We have still quantified, with sensitivity, the value of the energy transmitted by the light pipe. For example, in the clear sky, we noted a radiant flux (285 to 2800 nm) of nearly 7.5±3.5 W/m^2 inside, or less than 123 times the outdoor solar irradiance. This value allowed us to estimate the minimum luminous efficacy of the light pipe (taking into account the highest radiant flux) in a clear sky (591 $lm.W^{-1}$) and overcast sky (85.5 $lm.W^{-1}$), and then to compare them to the luminous efficacy of various sources. The latter shows a result nine times higher in the clear sky than a compact fluorescent lamp. The results for the 4500 nm to 42000 nm range (LW, IR) also show that the thermal impact of the mirrored light pipe is limited. The "quantitative" studies concern the measurements associated with the spectrophotometer covering the electromagnetic wave spectrum from 200 to 1100 nm. At the exit of the light pipe, no UV is detected, and the spectral profile of the transmitted light shows us a relatively continuous spectral irradiance in the visible range. This confirms the literature findings: the light pipe, in the clear sky as overcast, diffuses an achromatic light, unlike the artificial lighting source studied.

We show that this system is well suited to promote visual comfort thanks to its non-visual effects (intermittence of the luminous flux, chronobiology, and cognitive performance). It can provide full-spectrum light in spaces that have few or no openings in the front. These rooms typically use artificial lighting that does not regulate circadian rhythms. Our experimental work has shown that the light pipe brings little heat and does not modify the visible light spectrum, thus providing beneficial light for humans.

Our experimental study was conducted on a single type of mirrored light pipe (curve, with an aspect ratio of 4.6). These results allow us to understand the thermal and spectral behavior of the light pipe. The evolution of geometric parameters (different aspect ratios, straight rather than a curved light pipe) or photometric parameters (different reflection coefficient) will modify the number of light rays transmitted. The level of interior illuminance will also change. However, this should not affect the spectroscopic profile of the light passing through it. As found in the literature, the dominant parameter to act on the spectrum profile is the angle of incidence of the incoming rays. Further studies may confirm these hypotheses.

The light pipe is the most successful daylighting device to meet the growing need for bioclimatic design in a device focused on human well-being. The study of multimodal comfort would allow orienting technical innovations so that the building can adapt to the human being, and not the opposite.

5. Acknowledgment

The authors thank Mr. J. Vigneron for his help in taking the measurements. Thanks are also due to Mr. E. Jouen for his assistance in setting up the experiment and the loan of specific measuring equipment.

6. References

[1] Frontczak M, Wargocki P. Literature survey on how different factors influence human comfort in indoor environments. Build Environ 2011;46:922–37. https://doi.org/10.1016/j.buildenv.2010.10.021.

[2] Veitch JA, Erhan E, Gregory J. Office Light Source Spectrum: Effects of Individual Control on Perception, Cognition, and Comfort 2012.

[3] Prayag A, Münch M, Aeschbach D, Chellappa S, Gronfier C. Light Modulation of Human Clocks, Wake, and Sleep. Clocks & Sleep 2019;1:193–208. https://doi.org/10.3390/clockssleep1010017.

[4] Hatori M, Gronfier C, Van Gelder RN, Bernstein PS, Carreras J, Panda S, et al. Global rise of potential health hazards caused by blue light-induced circadian disruption in modern aging societies. NPJ Aging Mech Dis 2017;3:9. https://doi.org/10.1038/s41514-017-0010-2.

[5] Hicks D, Attia D, Behar-Cohen F, Carré S, Enouf O, Falcon J, et al. How good is the evidence that light at night can affect human health? Graefe's Arch Clin Exp Ophthalmol 2020;258:231–2. https://doi.org/10.1007/s00417-019-04579-6.

[6] Agence nationale de sécurité sanitaire de l'alimentation (Anses). Effets sur la santé humaine et sur l'environnement (faune et flore) des diodes électroluminescentes (LED) 2019:1–458. https://doi.org/10.13140/RG.2.2.35128.70406.

[7] Malet-Damour B, Bigot D, Boyer H. Technological Review of Tubular Daylight Guide System from 1982 to 2020. Eur J Eng Res Sci 2020;5:375–86. https://doi.org/10.24018/ejers.2020.5.3.1809.

[8] Malet-Damour B, Bigot D, Guichard S, Boyer H. Photometrical analysis of mirrored light pipe: From state-of-the-art on experimental results (1990–2019) to the proposition of new experimental observations in high solar potential climates. Sol Energy 2019;193:637–53. https://doi.org/10.1016/j.solener.2019.09.082.

[9] Malet-Damour B, Guichard S, Bigot D, Boyer H. Study of tubular daylight guide systems in buildings: Experimentation, modelling and validation. Energy Build 2016;129:308–21. https://doi.org/10.1016/j.enbuild.2016.08.019.

[10] Nilsson AM, Jonsson JC, Roos A. Spectrophotometric measurements and ray tracing simulations of mirror light pipes to evaluate the color of the transmitted light. Sol Energy Mater Sol Cells 2014;124:172–9. https://doi.org/10.1016/j.solmat.2014.01.049.

[11] Shao L, Riffat SB. Daylighting using light pipes and its integration with solar heating and natural ventilation. Int J Light Res Technol 2000;32:133–9. https://doi.org/10.1177/096032710003200305.

[12] Callow JM, Shao L. Air-clad optical rod daylighting system. Light Res Technol 2003;35:31–8. https://doi.org/10.1191/1477153503li081oa.

[13] Omishore A, Kalousek M, Mohelník P. Thermal testing of the light pipe prototype. Eng Rev 2019;39:283–91. https://doi.org/10.30765/er.39.3.09.

[14] Varga S, Oliveira AC. Ventilation terminals for use with light pipes in buildings: A CFD study. Appl Therm Eng 2000;20:1743–52. https://doi.org/10.1016/S1359-4311(00)00005-3.

[15] Oakley G. TripleSave – The Investigation and Monitoring of a Combined Natural Daylighting and Stack Ventilation System . Inst Build Technol Sch Built Environ Univ Nottingham 2001:1–18.

[16] Šikula O, Mohelníková J, Plášek J. Thermal CFD analysis of tubular light guides. Energies 2013;6:6304–21. https://doi.org/10.3390/en6126304.

[17] Šikula O, Mohelníková J, Plášek J. Thermal analysis of light pipes for insulated flat roofs. Energy Build 2014;85:436–44. https://doi.org/10.1016/j.enbuild.2014.09.044.

[18] Ait-taleb T, Abdelbaki A, Zrikem Z. Numerical simulation of coupled heat transfers by conduction, natural convection and radiation in hollow structures heated from below or above. Int J Therm Sci 2008;47:378–87. https://doi.org/10.1016/j.ijthermalsci.2007.01.035.

[19] Williams D, Jean-Francois D. Nvestigating the Thermal and the Lighting Performance of Light Pipes for Sunny and Cloudy Conditions in Insular Tropical Climate. Electr Eng 2014;2:7. https://doi.org/10.17265/2328-2223/2014.05.

[20] Harrison SJ, McCurdy R, Cooke R. Preliminary evaluation of the daylighting and thermal performance of

cylindrical skylights. Proc. Daylighting 98 - Int. Conf. daylighting Technol. energy Effic. Build., Ottawa: 1998, p. 205–12.

[21] Callow BJ. Daylighting Using Tubular Light Guide Systems. University of Nottingham, 2003.

[22] Laouadi A, Atif MR. Transparent domed skylights: Optical model for predicting transmittance, absorptance and reflectance. Int J Light Res Technol 1998;30:111–8. https://doi.org/10.1177/096032719803000304.

[23] McCluney R. Rating of Tubular Daylighting Devices for Visible Transmittance and Solar Heat Gain - Final Report. Cocoa, Florida: 2003.

[24] Bencs P, Szabó S, Oertel D. Simultaneous measurement of velocity and temperature field in the downstream region of a heated cylinder. Eng Rev 2014;34:7–13.

[25] Perčić M, Lenić K, Trp A. A three-dimensional numerical analysis of complete crossflow heat exchangers with conjugate heat transfer. Eng Rev 2013;33:23–40.

[26] Hien VD, Chirarattananon S, Luang K. Daylighting Through Light Pipe for Deep Interior Space of Buildings With Consideration Heat Gain. Asian J Energy Environ 2007;08:461–75.

[27] Wu Y, Yue Z. Experimental investigation on light-thermal effects of solar light pipes used in USTB gymnasium under sunny conditions in Beijing. 2009 Int. Conf. Energy Environ. Technol. ICEET 2009, vol. 1, 2009, p. 147–50. https://doi.org/10.1109/ICEET.2009.42.

[28] Dumortier D. Mesure, analyse et modélisation du gisement lumineux : Application à l'évaluation des performances de l'éclairage naturel des bâtiments. 1995.

[29] Kittler R. Luminance models of homogeneous skies for design and energy performance predictions. Proc. 1 St, Int. Daylighting Conf., 1986, p. 18–22.

[30] Perez R, Michalsky J, Seals R. Modeling sky luminance angular distribution for real sky conditions: Experimental evaluation of existing algorithms. J Illum Eng Soc 1992;21:84–92. https://doi.org/10.1080/00994480.1992.10748005.

[31] Perraudeau M. Luminance models. Natl. Light. Conf. daylighting Colloq., Cambridge: 1988, p. 291–292.

[32] Pattanasethanon S, Lertsatitthanakorn C, Atthajariyakul S, Soponronnarit S. All sky modeling daylight availability and illuminance/irradiance on horizontal plane for Mahasarakham, Thailand. Energy Convers Manag 2007;48:1601–14. https://doi.org/10.1016/j.enconman.2006.11.012.

[33] Fakra AH, Boyer H, Miranville F, Bigot D. A simple evaluation of global and diffuse luminous efficacy for all sky conditions in tropical and humid climate. Renew Energy 2011;36:298–306. https://doi.org/10.1016/j.renene.2010.06.042.

[34] Fakra AH, Boyer H, Miranville F, Bigot D. A simple evaluation of global and diffuse luminous efficacy for all sky conditions in tropical and humid climate. Renew Energy 2011;36:298–306. https://doi.org/10.1016/j.renene.2010.06.042.

[35] Brainard GC, Hanifin JR, Greeson JM, Byrne B, Glickman G, Gerner E, et al. Action spectrum for melatonin regulation in humans: Evidence for a novel circadian photoreceptor. J Neurosci 2001;21:6405–12. https://doi.org/10.1523/jneurosci.21-16-06405.2001.

[36] Rea MS, Figueiro MG, Bierman A, Hamner R. Modelling the spectral sensitivity of the human circadian system. Light Res Technol 2012;44:386–96. https://doi.org/10.1177/1477153511430474.

[37] Van Bommel W. Visual, biological and emotional aspects of lightings: Recent new findings and their meaning for lighting practice. LEUKOS - J Illum Eng Soc North Am 2005;2:7–11. https://doi.org/10.1582/LEUKOS.02.01.001.

[38] Cajochen C, Münch M, Kobialka S, Kräuchi K, Steiner R, Oelhafen P, et al. High sensitivity of human melatonin, alertness, thermoregulation, and heart rate to short wavelength light. J Clin Endocrinol Metab 2005;90:1311–6. https://doi.org/10.1210/jc.2004-0957.

[39] Vandewalle G, Maquet P, Dijk D-J. Light as a modulator of cognitive brain function. Trends Cogn Sci 2009;13:429–38. https://doi.org/10.1016/j.tics.2009.07.004.

[40] Boyce P, Hunter C, Howlett O. The Benefits of Daylight through Windows Sponsored by : Capturing the Daylight Dividend Program The Benefits of Daylight through Windows 2003:1–88.

[41] Phipps-Nelson J, Redman J, Sleep DD-, 2003 undefined. Daytime exposure to bright light, as compared to dim light, decreases sleepiness and improves psychomotor vigilance performance. n.d.

[42] Rüger M, M Gordijn MC. Article in AJP Regulatory Integrative and Comparative Physiology. ResearchgateNet 2006;290. https://doi.org/10.1152/ajpregu.00121.2005.

[43] Viola AU, Dijk D-J. Blue-enriched white light in the workplace improves self-reported alertness, performance and sleep quality. Artic Scand J Work 2008. https://doi.org/10.5271/sjweh.1268.

[44] Vandewalle G, Schmidt C, Albouy G, one VS-P, 2007 undefined. Brain responses to violet, blue, and green monochromatic light exposures in humans: prominent role of blue light and the brainstem. NcbiNlmNihGov n.d.

[45] Zeitzer JM, Dijk DJ, Kronauer RE, Brown EN, Czeisler CA. Sensitivity of the human circadian pacemaker to nocturnal light: Melatonin phase resetting and suppression. J Physiol 2000;526:695–702. https://doi.org/10.1111/j.1469-7793.2000.00695.x.